

Article

Effect of Thermal Bridges in Insulated Walls on Air-Conditioning Loads Using Whole Building Energy Analysis

Mohamed F. Zedan *, Sami Al-Sanea, Abdulaziz Al-Mujahid and Zeyad Al-Suhaibani

Mechanical Engineering Department, King Saud University, Riyadh 11421, Saudi Arabia; sanea@ksu.edu.sa (S.A.-S.); amujahid@ksu.edu.sa (A.A.-M.); zeyads@ksu.edu.sa (A.A.-S.)

* Correspondence: mzedan@ksu.edu.sa; Tel.: +966-50-895-4548

Academic Editor: Andrew Kusiak

Received: 13 April 2016; Accepted: 9 June 2016; Published: 16 June 2016

Abstract: Thermal bridges in building walls are usually caused by mortar joints between insulated building blocks and by the presence of concrete columns and beams within the building envelope. These bridges create an easy path for heat transmission and therefore increase air-conditioning loads. In this study, the effects of mortar joints only on cooling and heating loads in a typical two-story villa in Riyadh are investigated using whole building energy analysis. All loads found in the villa, which broadly include ventilation, transmission, solar and internal loads, are considered with schedules based on local lifestyles. The thermal bridging effect of mortar joints is simulated by reducing wall thermal resistance by a percentage that depends on the bridges to wall area ratio (TB area ratio or A_{mj}/A_{tot}) and the nominal thermal insulation thickness (L_{ins}). These percentage reductions are obtained from a correlation developed by using a rigorous 2D dynamic model of heat transmission through walls with mortar joints. The reduction in thermal resistance is achieved through minor reductions in insulation thickness, thereby keeping the thermal mass of the wall essentially unchanged. Results indicate that yearly and monthly cooling loads increase almost linearly with the thermal bridge to wall area ratio. The increase in the villa's yearly loads varies from about 3% for $A_{mj}/A_{tot} = 0.02$ to about 11% for $A_{mj}/A_{tot} = 0.08$. The monthly increase is not uniform over the year and reaches a maximum in August, where it ranges from 5% for $A_{mj}/A_{tot} = 0.02$ to 15% for $A_{mj}/A_{tot} = 0.08$. In winter, results show that yearly heating loads are generally very small compared to cooling loads and that heating is only needed in December, January and February, starting from late night to late morning. Monthly heating loads increase with the thermal bridge area ratio; however, the variation is not as linear as observed in cooling loads. The present results highlight the importance of reducing or eliminating thermal bridging effects resulting from mortar joints in walls by maintaining the continuity of the insulation layer in order to reduce energy consumption in air-conditioned buildings.

Keywords: thermal bridges; mortar joints; transmission load; R-value; wall thermal performance; building envelope

1. Introduction

Thermal bridges in the outer walls of buildings are typically caused by mortar joints between insulated building blocks and by concrete structural elements, such as columns, beams and slabs. These bridges create an easy path for heat transfer across the building envelope and usually result in increased heating and cooling loads in buildings. Accurate thermal bridging assessment is becoming extremely important not only in predicting peak thermal loads and yearly heating/cooling loads, but also in estimating the potential for condensation and subsequent mold growth in the heating season in

cold climates. The main difficulty in modeling thermal bridges stems from the fact that they create significant two-dimensional (2D) effects on heat transmission across building walls in the case of mortar joints and three-dimensional (3D) effects in the case of concrete structural elements. At the same time, most building energy simulation computer packages utilize one-dimensional models in order to simplify lengthy calculations.

The literature survey reported in the next section shows that most studies on thermal bridges consider mainly those caused by structural elements and that little attention was given to mortar joints. To remedy this deficiency, the present investigation deals with the effects of mortar joints in the walls of a typical villa. When using insulated building blocks, mortar joints cause discontinuities in the insulation layer along the wall height, as shown in Figure 1, and therefore provide little resistance to heat transmission compared to the insulation layer itself. This affects adversely the effectiveness of thermal insulation, resulting in considerable reduction in the R-value of the wall compared to a wall with a continuous insulation layer. Using a 2D dynamic model for heat transmission through a typical wall section with mortar joints, Al-Sanea and Zedan [1] showed that the reduction in the R-value depends on both the ratio of the thermal bridge area to wall area (TB ratio or A_{mj}/A_{tot}) and the insulation thickness (L_{ins}). In the present paper, we deal with a whole building (villa) rather than a wall section [1] to study the effects of thermal bridges on the hourly, monthly and yearly cooling and heating loads, under Riyadh ambient conditions. All loads found in a typical villa are considered using whole building energy analysis. These loads broadly include ventilation loads, solar loads, internal loads (lights, people, equipment, *etc.*, with typical schedules based on local lifestyles) and of course heat transmission through the villa's envelope, with the latter being the dominant load under Riyadh ambient conditions.

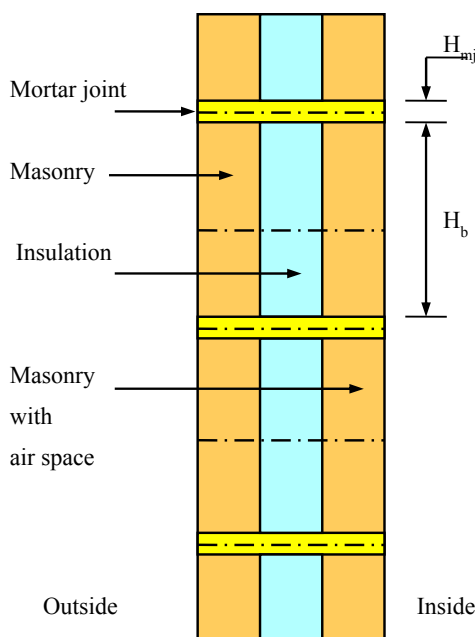


Figure 1. Diagrammatic sketch showing thermal bridges caused by mortar joints in building walls.

The thermal bridging effect resulting from mortar joints is simulated, in the present work, by reducing the wall thermal resistance (R-value) by a percentage that corresponds to the bridge to wall area ratio and the nominal thickness of the insulation layer. The percentage reduction in the R-value is obtained from a graphical correlation developed from detailed and rigorous 2D dynamic analysis of heat transmission through the same wall section that includes mortar joints, in a way similar to the study presented by the authors in Al-Sanea and Zedan [1]. The reduction in wall R-value is achieved by reducing the insulation thickness and thereby keeping the thermal mass of the wall essentially

unchanged. The whole building load simulation package used in the present investigation is the Hourly Analysis Program provided to the authors by the Carrier Corporation. This package, which is known as HAP [2], is based on ASHRAE load calculation procedures and is therefore extensively used by designers of air-conditioning systems and energy engineers worldwide for load estimation and building energy simulation. This package and two other commercial packages were validated in a doctoral dissertation [3] for an actual building at Iowa State University by comparison with measurements. Al-Tahat and Al-Ali [4] validated the HAP energy simulation feature by comparing the historical energy consumption data and simulation results of an existing building before applying any energy saving measures. The deviation between HAP results and actual data was within 5%.

The research background of thermal bridges is reviewed next, followed by a short description of the present case study. A summary of the 2D dynamic heat transfer model used to account for the effect of mortar joints on wall thermal resistance and to develop the correlation for these effects is given next. The results of the whole building energy analysis of the simulated effects of thermal bridges are then presented.

2. Research Background

Asdrubali *et al.* [5] proposed a quick and approximate methodology to perform quantitative analysis of thermal bridges, through thermographic surveys of the wall surface followed by analytical processing. From the simple measurement of the air temperature and the analysis of the thermograph, the thermal bridge effect can be estimated as a percentage increase over the same wall, but with homogenous transmittance. Ascione *et al.* [6] compared different methods for modelling thermal bridges created by flat heterogeneous concrete slabs in a multistory office building, as well as the results of energy simulation programs for Italian climates. The methods used are simplified 1D models with a homogeneous structure and more sophisticated 2D or 3D models. They concluded that proper modelling of thermal bridges is necessary. Hassid [7] presented an integral approach to calculate thermal bridge effects at the junction between dissimilar, multilayer walls. The model is based on the solution of the integrated 2D conduction equation for the main wall and the thermal bridge. The predicted overall heat transfer coefficients and minimum internal surface temperatures are shown to compare favorably with proper computational solution. However, this 2D model is limited to a steady state solution that ignores both solar radiation and long wave radiation at the outside surface.

Martin *et al.* [8] investigated the problems encountered in the calculation of thermal bridges under dynamic conditions considering their thermal inertia when using energy simulation programs. They pointed out the need for proper treatment as the TB effect becomes more pronounced at the high insulation thicknesses required by building codes in recent years. The study was carried out for thermal bridges with thermal inertia similar to the homogenous wall and for thermal bridges with much lower inertia. Martin with others [9] followed up on this study by carrying out a series of experiments in a guarded hot box testing facility to study the thermal response of pillar-type thermal bridges under both steady and dynamic conditions. One of the main objectives of this study was the determination of the influence of the area of the thermal bridge on heat transfer across building walls. The test results were compared to those obtained from building energy simulation. The authors pointed out that there is a great deal of uncertainty regarding the dynamic behavior of thermal bridges when using energy simulation programs. They concluded that proper treatment of thermal bridges and their *in situ* construction is necessary for calculating the overall thermal demand of buildings.

Evola *et al.* [10] presented a study on the effects of thermal bridges for two building types, terraced houses and semi-detached houses, considering three envelope designs commonly used in Italy for the mild Mediterranean climate. The buildings are characterized by a reinforced concrete structure and clay block walls. The thermal performance of the envelopes complies with Italian regulations for new construction. The impact of thermal bridges on both heating and cooling loads was studied first. Then, the economic value of correcting such thermal bridges, while considering additional costs of construction and refurbishment, was assessed by calculating the discounted payback period.

One of the methods the author considered to correct or reduce the effects of thermal bridges is to cover the whole wall by insulated boards. Unfortunately, the cost-benefit analysis has shown that the savings produced by rectifying thermal bridge effects are not sufficient to recover the additional costs of construction and refurbishment. However, one should realize that such a conclusion is valid for the methods that the authors used to reduce the effects of thermal bridges under mild Mediterranean climatic conditions and, therefore, should not be generalized.

Gao *et al.* [11] used state model reduction techniques to develop a low-order (reduced) three-dimensional heat transfer model by including terms for the additional losses/gains through thermal bridges in their analysis. The authors validated this model in both frequency and time domains. The model was then implemented in the software package “TRNSYS” resulting in a large reduction in the amount of calculations in time simulations. Ben-Nakhi [12] presented a dynamic thermal bridging assessment module that is integrated within a whole building simulation environment with more realistic boundary conditions. It integrates all inter-related energy subsystems that exist in buildings.

More recent studies by Bianchi *et al.* [13] and Cuce and Cuce [14] focused on experimental investigation to analyze thermal bridging effects. Bianchi *et al.* [13] carried out in-field experimental measurements in order to evaluate energy losses through the envelope of a test room. Infrared thermography and the so-called “incidence factor of thermal bridges”, proposed in a previous study by the same authors, were applied to assess the energy losses due to thermal bridges. The incidence factor of thermal bridges was based on indoor air temperature, surface temperature and thermal fluxes throughout the building envelope. This factor represented the ratio between thermal transmittance in the presence of a thermal bridge to that in its absence and could be considered as a thermal bridge correction factor. Results showed that the overall effect of thermal bridges in increasing thermal losses through the building envelope corresponded to about 9%. It is interesting to note that the current study adopts a similar approach in presenting the effects of thermal bridges, but with using whole building energy analysis. Cuce and Cuce [14] presented an experimental and statistical study for evaluating thermal bridges at internally retrofitted walls of a test room. It was concluded that the mere internal retrofit was not a decisive solution to reduce the heat loss from residential buildings if additional proper attention was not paid to non-insulated building elements.

Although expensive, vacuum insulation panels (VIPs) are characterized by very low thermal conductivity, compared to traditional insulating materials, and hence, can improve the thermal behavior of buildings, especially in the case of energy retrofitting [15]. However, VIPs require the manufacturing of prefabricated panels of a fixed shape/size, which means that their use in the building envelope involves the problem of joining the panels to each other and of fixing them onto additional supporting structures. The problem with this technique is that these structures and systems themselves cause thermal bridging effects. The energy performance of the resulting insulation package can therefore be affected to a great extent by these additional elements and can become significantly lower than that of the VIP panel alone. Using a heat flux meter, Lorenzati *et al.* [15] carried out experiments in order to verify the effect of thermal bridges on the energy performance of VIPs. Results were used to calibrate and verify a numerical model that allowed the performance of various VIP joint materials/typologies to be predicted and the performance of the overall package to be optimized.

Quinten and Feldheim [16] reviewed and tested different approaches for modeling the heat transfer through a thermal bridge with implementation into building energy simulation programs. The approaches were based on an equivalent wall method. The equivalent wall replaces the thermal bridge by having the same steady and dynamic thermal behavior as the thermal bridge. The authors proposed a new method, which was a mix between the principles of the structure factors method and a harmonic method. The mixed method was tested on a 2D thermal bridge, the junction between the floor and exterior wall, and was found to lead to accurate results and a unique solution. Martins *et al.* [17] assessed several thermal bridge mitigation strategies to improve the thermal performance of a lightweight steel-framed (LSF) wall module and to reduce energy consumption. The implementation of thermal bridges' mitigation strategies in a modular LSF wall was performed using 3D FEM models.

The implementation of those mitigation strategies led to a reduction of 8.3% in the U-value. An optimization of the wall module insulation layers was also performed, which, combined with the mitigation approaches, allowed a decrease of 68% in the U-value. Design rules for lightweight steel-framed elements were also presented.

Two international standards (EN ISO 10211 [18] and EN ISO 14683 [19]) are frequently referred to by researchers in this area. ISO 2011 [18] lays out the specifications for the 3D and 2D geometrical models of a thermal bridge for the numerical calculation of heat flows, in order to assess the overall heat loss from a building or part of it and the minimum surface temperatures, in order to assess the risk of surface condensation, assuming all physical properties are independent of temperature and no heat sources within the building element. International Standard ISO 14683 [19] deals with simplified methods for determining heat flows through linear thermal bridges that occur at junctions of building elements. Furthermore, it specifies manual calculation methods related to thermal bridges. Unfortunately, the thermal bridges covered in these two standards are those caused by structural elements and not by mortar joints.

In summary, as was mentioned in the Introduction, the research background showed that most previous studies on thermal bridging effects focused on bridges caused by structural elements and that little attention was given to mortar joints. The present study quantifies the effects of mortar joints in building walls on whole building energy consumption through modifying the conductive wall thermal resistance. It is noted that the thermal inertia per unit mass of the mortar joints is effectively the same as the bulk masonry.

3. Description of the Case Study

3.1. General

The building under consideration is a two-story villa (detached home) located in Riyadh. The total floor area is 400 m² (200 m² each level). The building plans for the villa are shown in Figure 2. The ground floor of the villa consists of a formal reception area, formal dining room, family room, toilets and kitchen. The first floor consists of four bedrooms, a living space/games area and bathrooms. The remaining overall building characteristics are: average ceiling height = 2.8 m above the floor, roof height of about 5.6 m above the grade level, 16 windows (two on each of the north, south, west and east sides per floor) and two doors, one on the east side and another on the south side. A full description of the wall construction, roof construction and window construction, as well as their thermal properties is given in the next few sections. This is followed by energy simulation data.

3.2. Wall and Roof Construction

Figure 3 shows the construction of villa walls, which are basically built of insulated building blocks commonly used in Saudi Arabia and covered by two layers of plaster. The thickness of the insulation layer in the block L_{ins} is 75 mm and made of molded polystyrene. Please note that the figure shows a cyclic part of the wall section that is repeated along the wall height. A photograph of the type of block modeled is shown in Appendix A. The roof construction is shown in Figure 4. Note that the insulation material for the roof is high-density molded polystyrene with a thickness $L_{ins} = 48$ mm. The properties of the wall and roof materials are shown in Table 1 below. The properties of the masonry materials are obtained mostly from the ASHRAE Handbook of Fundamentals [20]. The properties of the insulating materials vary according to the type of material and depend on many other factors, such as density, moisture content, temperature, aging, storage conditions, etc. The properties of molded polystyrene given in Table 1 for the walls and roof are specific to materials produced by local Saudi manufacturers as measured at room temperature by Al-Kasmoul [21]. It is interesting to note that the densities of insulation materials used in roofs are commonly higher than the densities of the same type of insulation materials used in walls in order to withstand higher pressure. Accordingly, the thermal

conductivities (as well as the costs) are different between the same type of insulation materials used in roofs and walls.

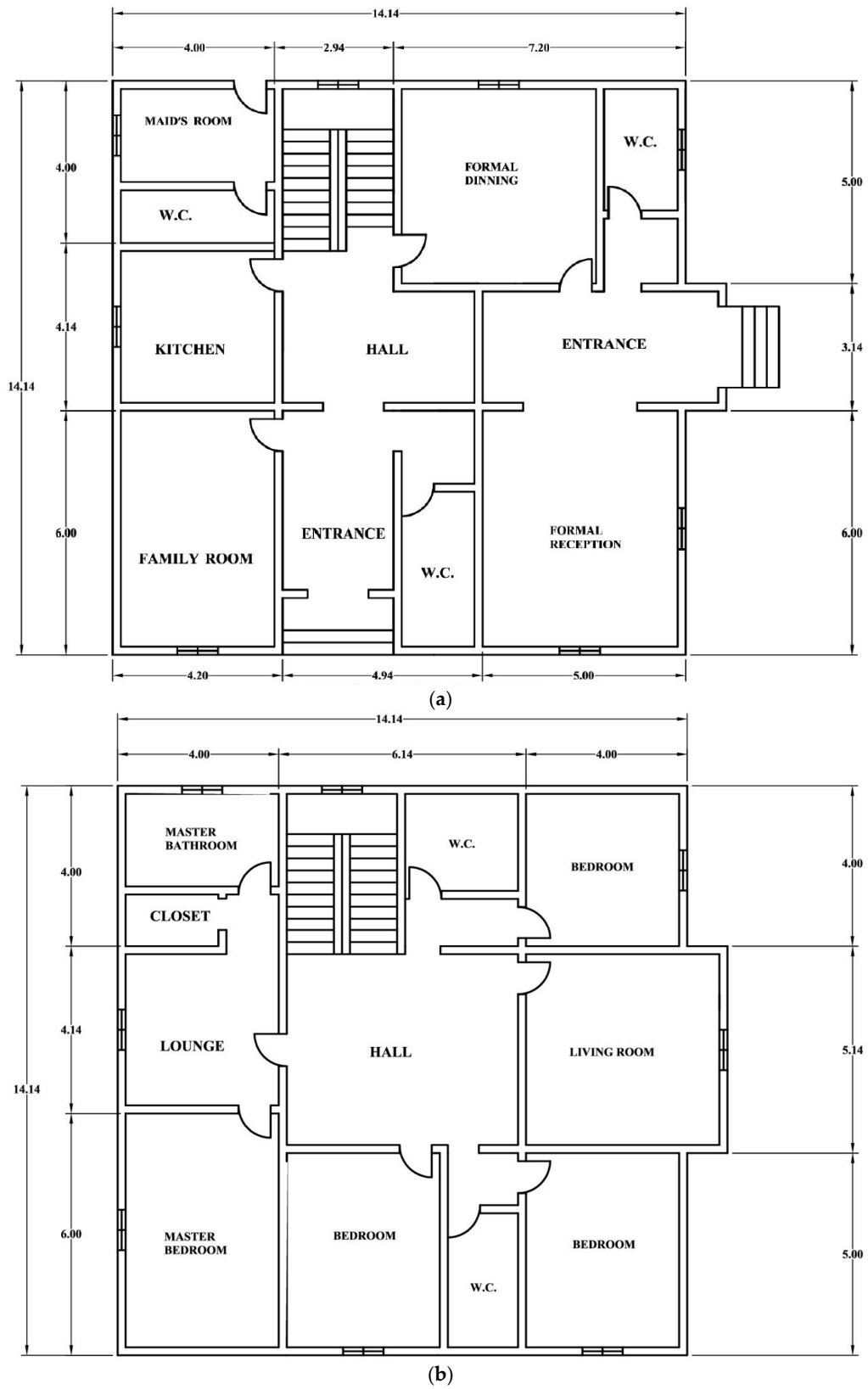


Figure 2. Building plans of the villa case study. (a) Ground floor plan; (b) first floor plan.

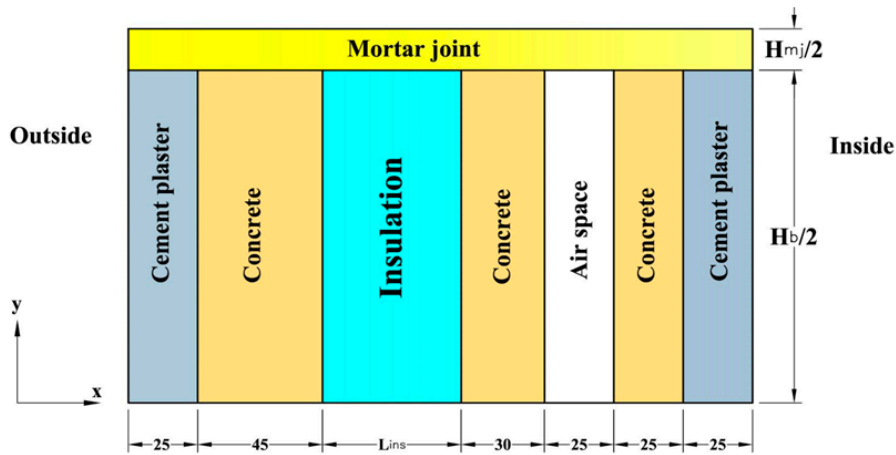


Figure 3. Cyclic part (symmetric region) of wall structure showing a five-layer building block covered by two cement plaster layers and a mortar joint cutting across the block; dimensions in mm.

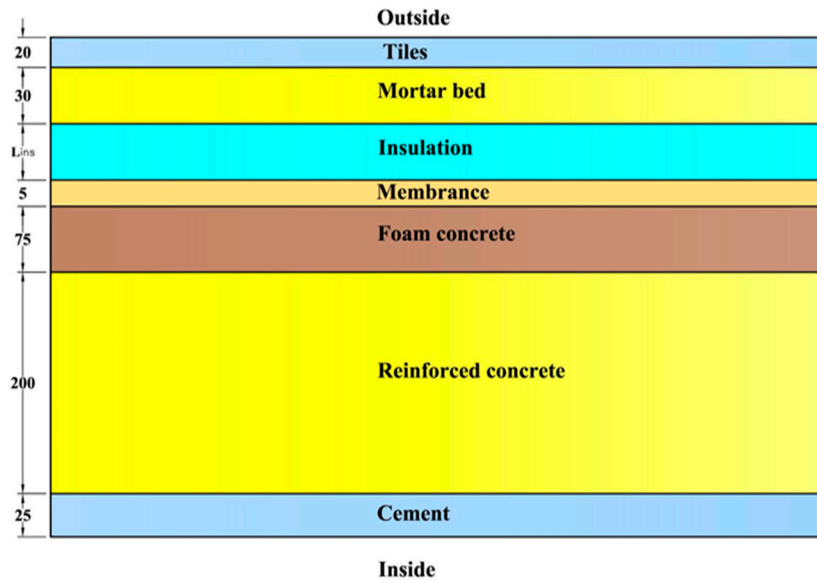


Figure 4. Schematic of a vertical roof section showing various layers (Dimensions. in mm, NTS).

Table 1. Wall and roof material properties [20,21].

Material	k (W/m·K)	ρ (kg/m ³)	c (J/kg·K)
Cement plaster	0.72	1860	840
Concrete	1.73	2243	840
Molded polystyrene (wall)	0.034	23	1280
Air space	$k_{eff} = 0.167$	1.1	1007
Molded polystyrene (roof)	0.033	38	1280
Tiles	0.84	1900	840
Mortar bed	0.72	1860	840
Membrane	0.5	1700	1000
Foam concrete	0.2	640	840
Reinforced concrete	2.3	2411	800
Heavyweight concrete	1.73	2243	840

3.3. Window Data

All windows are identical with the following data:

Dimensions: $W = 0.91 \text{ m (3 ft)} \times H = 1.52 \text{ m (5 ft)}$

Frame type: aluminum with thermal breaks

Internal shading: drapes, open weave, medium

Overall shading coefficient = 0.54

Overall U-value = $3.1 \text{ W/m}^2 \cdot \text{K}$

Glazing: double pane with a 6-mm air-space:

Outer glazing: a 3-mm gray tint with 0.631 transmissivity, 0.06 reflectivity and 0.304 absorptivity

Inner glazing: 3 mm, clear, with 0.841 transmissivity, 0.078 reflectivity and 0.081 absorptivity

3.4. Other Energy Simulation Data

With regard to weather conditions, HAP provides simulation weather data covering one full year for a large number of cities around the world, including Riyadh, as a built-in feature. These weather data are obtained from the IWEC (*International Weather Year for Energy Calculation*) data files released by ASHRAE in 2000 [22]. These datasets contain “typical” weather data intended for use with building energy simulation programs. The IWEC datasets utilize 18 years of hourly data by the National Climatic Data Center for 227 locations outside the USA and Canada. The international climatic zone number for Riyadh is one. The cooling degree days (CDD) are about 3500 °C and the heating degree days (HDD) are 410 °C for 18 °C base temperature.

Figure 5 shows the temperature and solar-radiation profiles during the month of August, as an example.

The villa building is supported by a concrete slab that sits on the ground (slab on grade). The area of the slab is 200 m², and its perimeter is 56.7 m. The exchange of heat between the indoor air within the ground floor and the soil occurs through the slab. This has been taken into consideration in the software. The U-coefficient for the slab is 0.568 m² · K/W.

The indoor temperature set points are: 23 °C for cooling and 22 °C for heating. The input data for internal heat gains are specified for each internal source (people, lighting, equipment, such as TVs, cooking appliances, computers, *etc.*) with its own specific schedule. These data are summarized as follows: six people (sedentary) in the villa; 2000 W lighting, 600 W equipment and 4000 W kitchen on the ground floor, in addition to 800 W lighting and 300 W TV on the first floor.

The input data for ventilation, with regard to the outdoor air requirements, are taken according to the ASHRAE STD 62.1–2007 [23], using values for residential dwelling unit. These values are 2.5 L/s per person and 0.3 L/s per square meter of floor area. This results in a 150-L/s ventilation rate, which was fixed throughout the year to ensure good indoor air quality via the constant volume AC system described later. For building weight input data, HAP offers options for light, medium and heavy construction. Although it is possible to specify values in between, we selected heavy construction since this is the closest to our case.

Regarding the selected HVAC system, there are a number of equipment options available for the air-conditioning of a typical villa in Riyadh. The system chosen for the villa under consideration is a roof-top packaged unit for cooling with an air-source heat pump for heating. In such a unit, all HVAC equipment is in one package from which conditioned air is fed to various spaces in the villa via a simple duct system ending with simple diffuser(s) in each space. Such a system is fairly common in above-average and upscale villas in Riyadh. The air distribution system is a constant volume system. Cooling capacity is controlled by cycling the compressor on and off, via a thermostat, while the fan is kept on as long as the system is on. Since our concern is the effect of thermal bridges in a typical Saudi home and not the air conditioning (AC) system design, the villa is treated as one single AC zone, which by the way, is the case in most existing villas with constant volume systems. Of course, one will have better control of temperature with a multi-zone system; however, constant volume multi-zone systems are energy inefficient because of using reheating to control temperature in various zones.

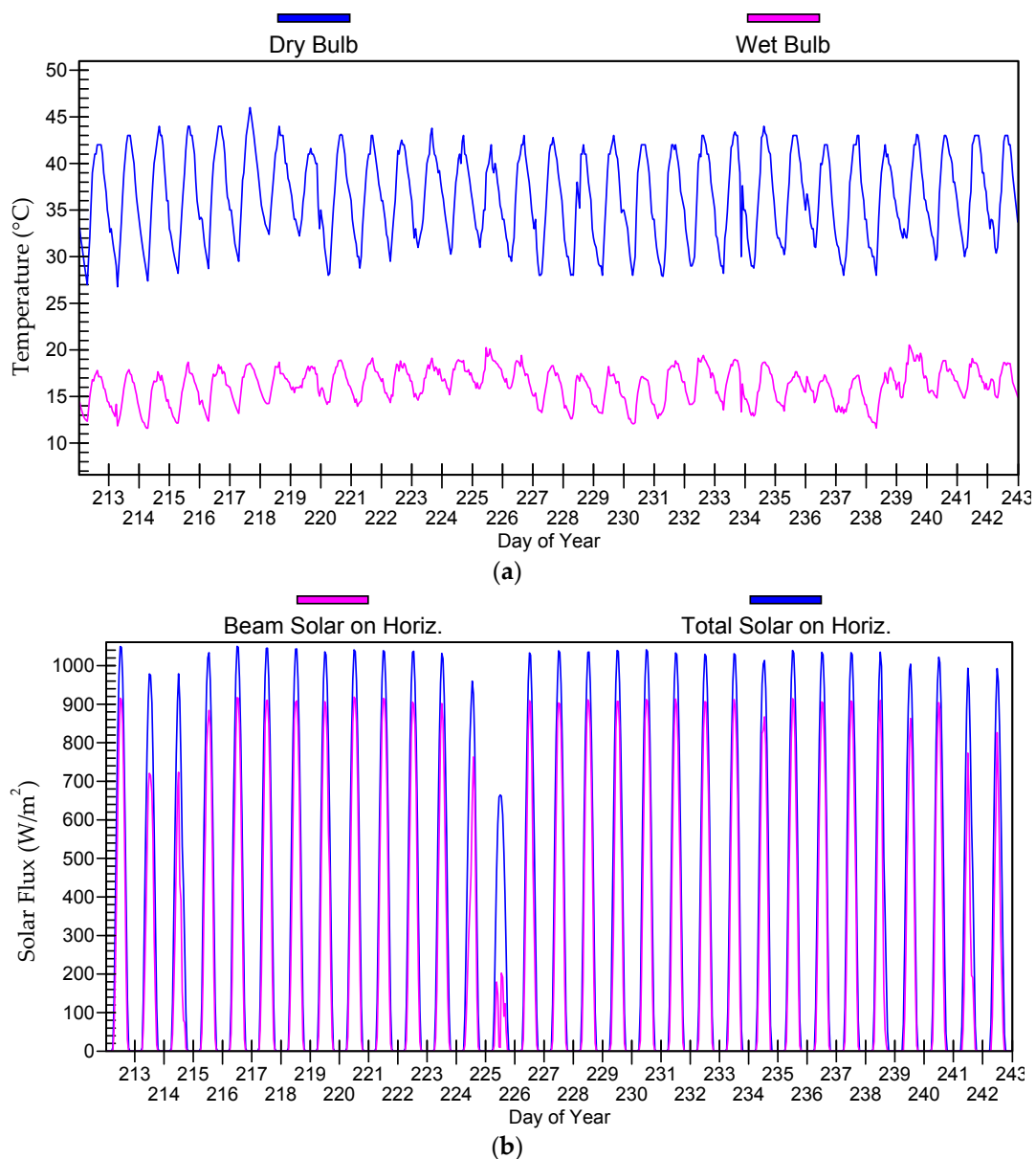


Figure 5. Riyadh sample weather data used in the simulation: 1 August (Day 213) through 31 August (Day 243). (a) Dry-bulb and wet-bulb temperature profiles; (b) Profiles of Solar flux on a horizontal plane.

4. Simulation of Effects of Thermal Bridges Using a 2D Dynamic Heat Transfer Model

The effect of the thermal bridges is simulated in the whole building analysis by reducing the wall thermal resistance by a percentage that depends on the thermal bridge to wall area ratio (A_{mj}/A_{tot}) and on the nominal thickness of thermal insulation (L_{ins}). These % reductions are obtained from studying the heat transfer across the wall with and without thermal bridges under 2D dynamic steady periodic conditions using a model developed previously by the first two authors. This model is detailed in Al-Sanea and Zedan [1] and is summarized, for completeness, in the next section.

4.1. Two-Dimensional Dynamic Model for a Wall with Thermal Bridges

In this section, we present only the main features of the model. Figure 1 shows the overall wall section where mortar joints cut across the insulation layer causing the thermal bridge, while Figure 3

shows a symmetric (cyclic) region of the wall section with all details. This symmetric region, which is repeated along the wall height, has a bottom symmetry plane passing through the middle of the building block and a top symmetry plane passing through the middle of the mortar joint. The outside surface of the wall is exposed to convection heat transfer ($q_{c,o}$), long wave radiation exchange with surroundings ($q_{r,o}$) and solar radiation (I_s). The inside surface is exposed to combined convection and radiation (q_i) heat transfer, which represent the rate of heat transmission into the inner space (transmission load).

For no heat generation, constant properties, 2D and negligible interface resistance, the equation governing time-dependent heat flow in the composite structure shown in Figure 3 is reduced to the Poisson equation, namely:

$$\frac{\partial}{\partial x} \left(k_j \frac{\partial T_j}{\partial x} \right) + \frac{\partial}{\partial y} \left(k_j \frac{\partial T_j}{\partial y} \right) = (\rho c)_j \frac{\partial T_j}{\partial t} \quad (1)$$

where the subscript j refers to wall layers (*i.e.*, $j = 1, 2, \dots, N$). The sought after solution of Equation (1) is $T(x,y,t)$, where x is the coordinate normal to wall layers and y is the coordinate along the wall height, as shown in Figure 3. The solution $T(x,y,t)$ requires an initial condition and boundary conditions at all boundaries. All layers are assumed to be initially at the mean ambient temperature, T_0 .

$$T_j(x,y,0) = T_0 \quad (2)$$

The steady periodic solution is independent of T_0 . The boundary conditions are as follows:

$$-k_N \left. \frac{\partial T}{\partial x} \right|_{x=L} = h_i (T_{x=L} - T_{f,i}) \quad (3)$$

at the inside surface where layer N lies on the inside, k_N is the thermal conductivity of layer N , h_i is the inside surface combined convection and radiation heat transfer coefficient, $T_{f,i}$ is the indoor air temperature, and:

$$-k_1 \left. \frac{\partial T}{\partial x} \right|_{x=0} = h_{c,o} (T_{f,o} - T_{x=0}) + \lambda I_s + q_{r,o} \quad (4)$$

at the outside surface, where Layer 1 lies on the outside, k_1 is the thermal conductivity of Layer 1, $h_{c,o}$ is the outside surface convection coefficient, $T_{f,o}$ is the outdoor air temperature and λ is the solar absorptivity.

At the planes of symmetry ($y = 0$ and $y = H$), the temperature gradient normal to either plane is zero, *i.e.*,

$$\left. \frac{\partial T}{\partial y} \right|_{y=0} = \left. \frac{\partial T}{\partial y} \right|_{y=H} = 0 \quad (5)$$

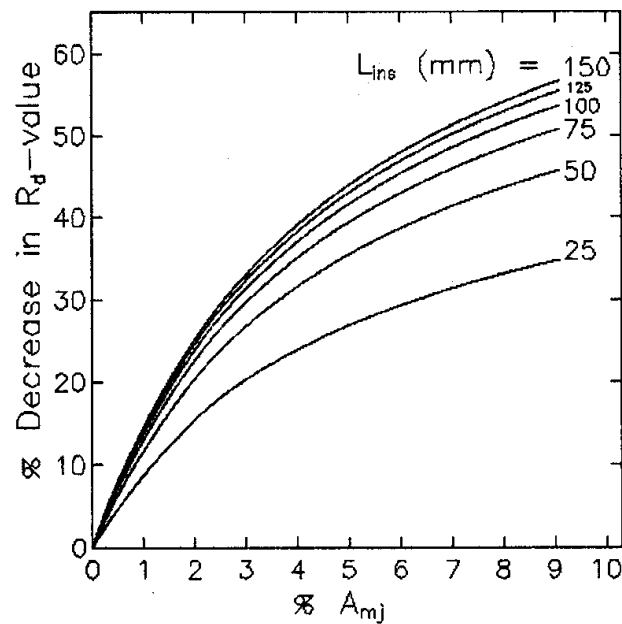
Equation (1) is solved numerically by a computer. Details of the numerical model and the computer solution of the above equations are given in Al-Sanea and Zedan [1].

4.2. Results of the 2D Dynamic Thermal Bridge Model

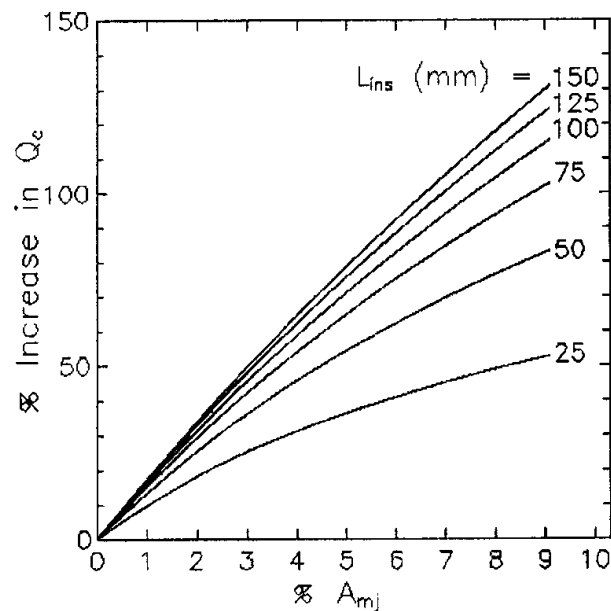
The above model was run for the wall shown in Figure 3 with different TB area ratios for a single nominal insulation thickness in a previous investigation [1]. In the present study, this work is extended to cover various nominal insulation thicknesses in order to obtain a more generalized correlation for the effect of thermal bridges under 2D dynamic conditions. Such a correlation would be useful for use in the future for wall structures similar to the present wall, but with different insulation thicknesses.

The results for the transmission load are obtained from the numerical solution on an hourly basis over a full year. The hourly results are integrated to obtain the transmission load on a monthly and yearly basis. The percentage increase in the yearly transmission load over the corresponding load without thermal bridges is shown in Figure 6a *versus* the TB percentage area ratio % A_{mj} for different nominal insulation thicknesses L_{ins} . Please note that % A_{mj} is basically $100 \times A_{mj}/A_{tot}$, where

A_{mj}/A_{tot} = mortar joint height H_{mj} divided by the block height H_b . The results in the figure show that the % increase in transmission load increases with the TB area ratio as expected for a given L_{ins} and increases with L_{ins} for a given TB area ratio. This confirms observations by previous investigators that higher insulation thicknesses accentuate the effects of thermal bridges [8]. The increase in transmission load as a result of thermal bridges is equivalent to a drop in the dynamic R-value of the wall. The corresponding correlation for the reduction in R-values is shown in Figure 6b. The results in that figure indicate that the drop in R-values increases with the TB area ratio for a given value of L_{ins} and increases with L_{ins} for a given TB area ratio and that such a drop can reach more than 50%.



(a)



(b)

Figure 6. Two-dimensional study results for the effect of % thermal bridge (TB) area ratio for various nominal insulation thicknesses: (a) percentage increase in yearly heat transmission load; (b) percentage decrease in yearly-averaged dynamic thermal resistance.

4.3. Utilization of the 2D Dynamic Thermal Bridge Model Results in Whole Building Simulation

The thermal bridging effect resulting from mortar joints is simulated, in the present whole building analysis, by reducing the wall thermal resistance (R-value) by a percentage that corresponds to the bridge to wall area ratio and the nominal thickness of the insulation layer. The percentage reduction in the R-value is obtained from the graphical correlation developed from the 2D dynamic analysis described above and presented in Figure 6b.

In the whole building energy analysis of the villa reported in the next section, the values for the percentage reduction in the wall R-values are picked up from the curve representing the 75-mm insulation thickness (in Figure 6b), which is the value of L_{ins} in the villa's walls. One of the most convenient ways to simulate the reduction in the R-value of the wall in whole building analysis is by reducing the thickness of the insulation layer. This is the route selected in the present study in order not to alter the wall thermal mass and therefore not to affect the dynamic characteristics of the original wall. The simulation program is run with the input data described in Section 3 previously and with walls having a 75-mm insulation thickness in order to establish the baseline case of no thermal bridges ($A_{mj}/A_{tot} = 0$) for this investigation. The simulation is then run multiple times, each time representing a different TB area ratio (A_{mj}/A_{tot}). Different TB area ratios are represented in the simulation via adjusting the insulation thickness to a value that corresponds to the A_{mj}/A_{tot} ratio for which the run is made, as shown in Table 2.

Table 2. Adjusted insulation thicknesses for simulating thermal bridge effects.

A_{mj}/A_{tot}	% Reduction in R-value (from 2D Correlation in Figure 6b)	$R_{adjusted}$ ($m^2 \cdot K/W$)	$L_{ins, adjusted}$ (mm)
0 (Baseline case)	0	2.660	75.00
0.02	22.5	2.062	54.65
0.04	35.0	1.729	43.35
0.06	42.9	1.519	36.20
0.08	48.5	1.370	31.14

It is interesting to note here that the effective R-value of the wall drops from 2.66 to 1.37 $m^2 \cdot K/W$ as a result of mortar joints with an area ratio of 8%. Because of the small density of polystyrene compared to other wall layers, the changes in wall thermal mass are negligibly small for the insulation thickness adjustments reported in Table 2.

The value of the thermal resistance for walls as recommended by the Saudi Building Code (SBC-Section 601, Energy Conservation), is obtained from a chart provided in the code at the degree days of Riyadh (CDD = 3500). The U-coefficient obtained from the chart is 0.7 $W/m^2 \cdot K$, which corresponds to an R-Value of 1.43 $m^2 \cdot K/W$. The R-values in the above table exceed this value, except for the case with a TB ratio of 0.08.

4.4. Representative Results of the Whole Building Energy Simulation

Before running the energy simulation, we have to make a design run to obtain the design load for each value of the thermal bridge ratio. Design cooling loads are summarized in Table 3 below.

The maximum value for the cooling load per unit area is 53.1 W/m^2 , or 18.8 m^2/kW (66 m^2/TR). We could not find any Saudi standards that stipulate target loads per unit area and classify residential building efficiency accordingly. However the above values indicate a highly efficient building when compared with some rules of thumb used by some engineers for rough estimate of loads based on area.

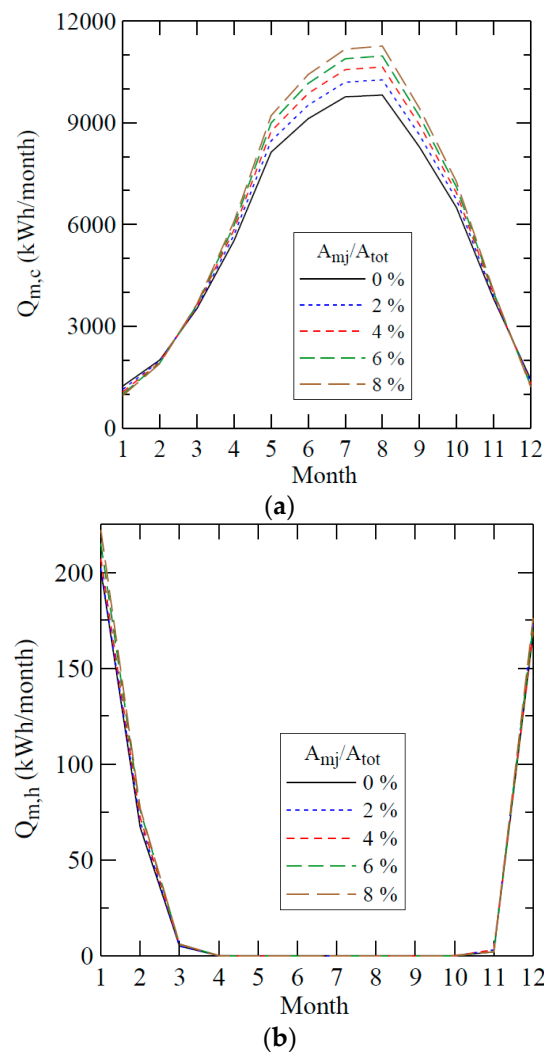
After design runs were made, the simulation feature of HAP was run on an hourly basis for one full year. Sample results are presented next; for more details and for the villa's daily and hourly cooling and heating loads, the reader may refer to Al-Sanea *et al.* [24].

Table 3. Design cooling loads of the villa building as obtained from HAP.

A_{mj}/A_{tot}	Design Cooling Load (kW)		Design Cooling Load per Unit Floor Area (W/m ²)	
	Coil	Space	Coil	Space
0 (Baseline case)	19.3	13.9	48.3	34.8
0.02	20.0	14.4	50	36
0.04	20.4	14.9	51	37.2
0.06	20.9	15.3	52.1	38.2
0.08	21.3	15.6	53.1	39

4.5. Monthly Cooling and Heating Loads

The monthly cooling and heating loads (in kWh) for the whole villa are shown in Figure 7a,b, respectively. It is obvious that the heating loads are much smaller than the cooling loads as expected in Riyadh and that heating is basically needed from December to February while cooling is needed over the whole year. As for the simulated effect of thermal bridges, the results in Figure 7 show that the bigger the thermal bridge area ratio (A_{mj}/A_{tot}), the higher the load. The biggest increase caused by the bridges occurs in August, which is the worst time for this to occur for both the utility company and the consumer because this is the time of year when the peak loads and peak energy consumption occur.

**Figure 7.** Villa's monthly loads for different thermal bridge area ratios. (a) Cooling; (b) heating.

4.6. Daily Cooling and Heating Loads

Sample results are presented for only two months; namely August (cooling) and January (heating). Figure 8 shows the daily cooling loads during the month of August. It is obvious that the daily loads increase with increasing thermal bridge area ratio, as expected. The corresponding results for the daily heating loads are shown for the month of January in Figure 9. Apart from using different ordinate scales on these two drawings, it is obvious that heating loads are generally much smaller than the cooling loads, which is typical under Riyadh outdoor weather conditions. Furthermore, one may observe that the effect of thermal bridges on the heating load is less pronounced than in the case of cooling in August.

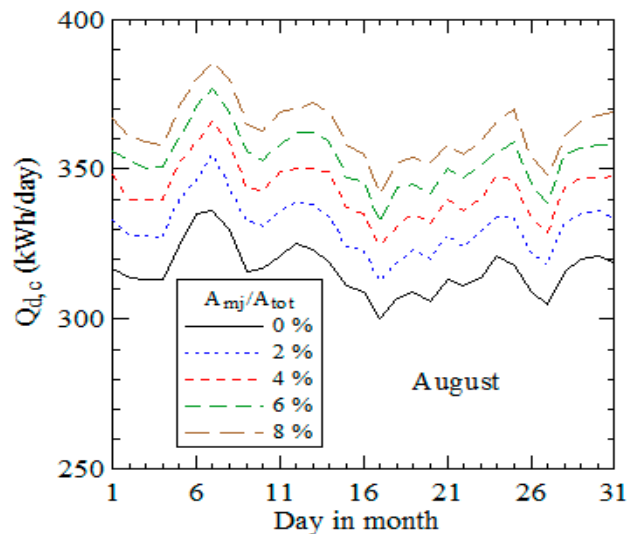


Figure 8. Villa's daily cooling loads in August for different thermal bridge area ratios.

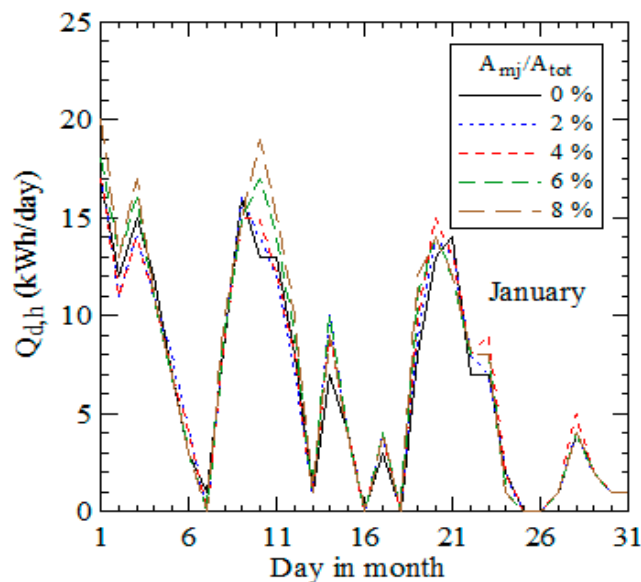


Figure 9. Daily heating loads in January for different thermal bridge area ratios.

4.7. Effect of Thermal Bridge Area Ratio on August and January Monthly Loads

The results presented in Figure 7 for the monthly cooling loads are recast by plotting the monthly load *versus* the A_{mj}/A_{tot} area ratio to show the effect of thermal bridges in a more explicit way.

Figure 10 shows such data for August. The results clearly indicate that the cooling load increases with A_{mj}/A_{tot} in an almost linear fashion. The increase in the August total monthly cooling load ranges between 4.6% for $A_{mj}/A_{tot} = 0.02$ and 14.7% for $A_{mj}/A_{tot} = 0.08$ when compared to the case with no thermal bridges.

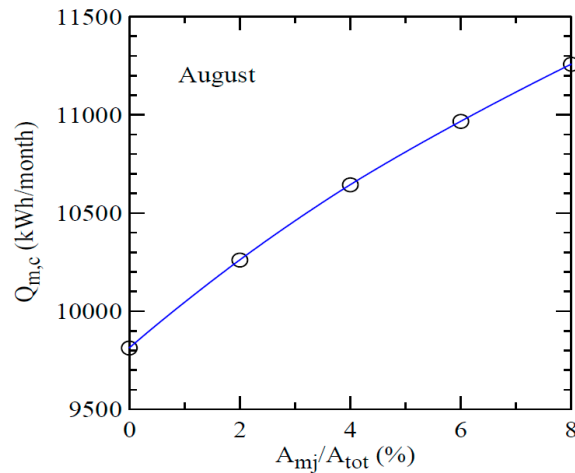


Figure 10. Effect of thermal bridges on August cooling load.

The corresponding results for the month of January are shown in Figure 11a for cooling and Figure 11b for heating. It may appear counter intuitive that cooling is needed in January, but there are days where the outdoor temperature is moderately cold, thereby reducing the heat loss from the villa envelope to a level just below internal heat gains, therefore requiring some cooling. The results in Figure 11a indicate clearly that the monthly cooling load in January drops monotonically and almost linearly with A_{mj}/A_{tot} as larger thermal bridges enhance heat loss through the walls, thereby reducing the cooling load. The reduction in the cooling load ranges from 7.9% for $A_{mj}/A_{tot} = 0.02$ to 22.9% for $A_{mj}/A_{tot} = 0.08$. These results indicate that higher thermal bridge area ratios have a beneficial effect in January, as they reduce cooling loads, which is the opposite of the trend observed in August. As for the heating load, the results in Figure 10b show that it increases with the thermal bridge area ratio, as expected, because larger thermal bridges increase heat loss from the villa and, therefore, increase the heating load on the HVAC equipment. However, the behavior is not quite as linear as we have seen in the cooling loads.

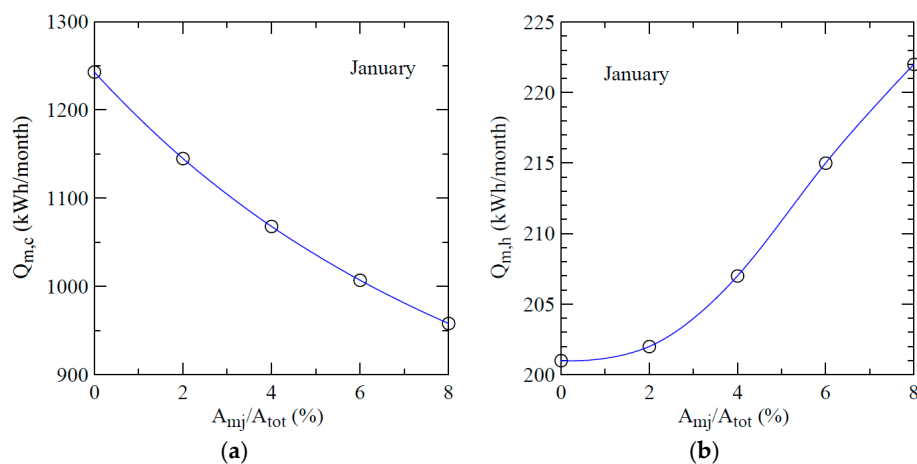


Figure 11. Effect of thermal bridges on January cooling and heating loads. (a) Cooling; (b) heating.

4.8. Effect of Thermal Bridge Area Ratio on Yearly Cooling and Heating Loads

The effect of A_{mj}/A_{tot} on the yearly cooling load of the villa is shown in Figure 12a. The load increases almost linearly with A_{mj}/A_{tot} . The yearly load ranges from 69,161 kWh/year at $A_{mj}/A_{tot} = 0$ to 76,624 kWh/year at $A_{mj}/A_{tot} = 0.08$. The increase in the yearly load compared to the case with no thermal bridges ranges from 2.9% for $A_{mj}/A_{tot} = 0.02$ to 10.8% for $A_{mj}/A_{tot} = 0.08$. The corresponding results for the yearly heating load are shown in Figure 12b. Although the load increases monotonically with A_{mj}/A_{tot} , the behavior is not as linear as in the cooling load. The yearly heating load increases from 443 kWh/year without thermal bridges to 482 kWh/year with thermal bridges of area ratio $A_{mj}/A_{tot} = 0.08$, representing an increase of about 9%. The nonlinear behavior of the heating load may be attributed to the fact that internal heat gains tend to reduce the heating load and that these loads are not uniform as they change according to specific schedules.

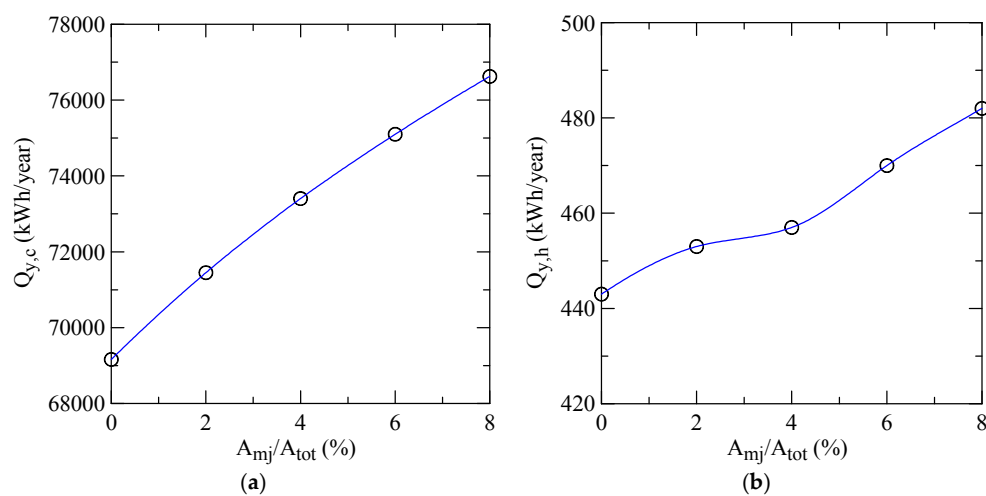


Figure 12. Effect of thermal bridges on yearly loads. (a) Cooling; (b) heating.

4.9. Energy Savings and Environmental Advantages of Eliminating Thermal Bridges

The effects of thermal bridges resulting from mortar joints can be eliminated by using tongue and groove insulated building blocks. In this configuration, the thermal insulation layer protrudes from one side of the block (tongue) with a corresponding recess on the other side of the block (groove). When these blocks are stacked above each other in a wall, the tongue engages into the groove thereby ensuring the continuity of the insulation layer. For a typical 1.2-cm mortar joint with a typical 20-cm height of insulated block (TB ratio of 0.06), the results of the yearly cooling and heating loads and the associated yearly electric loads (for HVAC equipment only) are in Table 4 below.

Table 4. Yearly cooling, heating and associated electric equipment loads for a TB ratio of 0.06 compared to the case with no thermal bridges.

TB Area Ratio	R-Value (m ² ·K/W)	Cooling Load (kWh/year)	Heating Load (kWh/year)	Cooling Electric Energy Consumption (kWh/year)	Heating Electric Energy Consumption (kWh/year)	Fan Electric Energy Consumption (kWh/year)	Total Electric Energy Consumption (kWh/year)
0.0	2.66	68,913	443	16,794	96	11,942	28,832
0.06	1.52	74,936	470	18,219	114	13,123	31,456

Based on Table 4 above, the electric energy savings brought about by eliminating mortar joint thermal bridges is 2624 kWh per year for this villa alone. The estimated number of residential units in Riyadh is about 960,000 [25]. Villas represent about 60% of residential units, while apartments represent about 40%. The floor area of the average apartment is about 40% of that of the villa. Therefore, the

saving weighing factor of a residential unit is $0.6 \times 1 + 0.4 \times 0.4 = 0.76$, *i.e.*, the saving per residential unit on average is $0.76 \times$ the savings per villa. This would translate to yearly energy savings of 1914 million kWh of electricity in the city of Riyadh alone.

According to the U.S. Energy Information Administration [26], 1 kWh of generated electricity produces 1.22 pounds of CO₂ emissions from plants energized by natural gas and 1.64 pounds for plants energized by distillate oil. Assuming roughly equal use of both fuels in Saudi Arabia, the average emissions per kWh generated is estimated to be 1.43 pounds. Further assuming about 10% losses in the transmission and distribution network, the amount of CO₂ that could be saved by eliminating mortar joint thermal bridges is estimated at 1.38×10^6 tons CO₂ per year, and this is for the city of Riyadh alone.

5. Summary and Concluding Remarks

The effects of thermal bridges in insulated building walls on the yearly, monthly and daily cooling and heating loads in a typical villa in Riyadh were investigated by using a commercial whole building energy simulation computer package (HAP). The thermal bridges considered in this study are solely due to mortar joints between insulated building blocks. The villa has two levels with a total floor area of 400 m² with all walls exposed to the ambient environment (detached home). All HVAC loads found in such a typical villa were considered with schedules based on local lifestyles. The thermal bridge effect was simulated in the whole building energy analysis by reducing the wall thermal resistance by a percentage that corresponds to the bridge to wall area ratio and the nominal thickness of the insulation layer. These percentage reductions were obtained from a graphical correlation developed based on the detailed and rigorous 2D dynamic analysis of mortar joint effects on heat transmission through wall sections.

The results indicate that the yearly cooling load of the villa increases almost linearly with the TB area ratio (A_{mj}/A_{tot}). The increase varies from about 3% for $A_{mj}/A_{tot} = 0.02$ to about 11% for $A_{mj}/A_{tot} = 0.08$. On a monthly basis, the variation of the cooling load with A_{mj}/A_{tot} is also approximately linear; however, the rate of increase is higher during summer months. In August, for example, the monthly cooling load increases by about 5% for $A_{mj}/A_{tot} = 0.02$ up to about 15% for $A_{mj}/A_{tot} = 0.08$. In winter, results show that heating is required mainly in December, January and February, starting from late night to late morning, while cooling is required from roughly noon time to late in the evening on some days. The heating loads are generally very small compared to the cooling loads in spite of cold outdoor weather in January, for example, because of internal heat generation from various sources within the villa. The results show further that the monthly heating load for that month increases with the thermal bridge area ratio; however, the variation is not as linear as observed earlier. The same behavior is observed for the yearly heating loads. It should be noted, however, that people seldom use mechanical cooling in winter in Riyadh; instead, they employ natural ventilation by allowing cold outdoor air into inhibited spaces to absorb heat generated indoors, but this was not considered in this study.

Because yearly heating loads are generally insignificant compared to cooling loads, the percentage effects of thermal bridges on heating reported earlier in the text may cause unwarranted concern. One should keep in mind that the absolute values of those effects (on heating) are almost negligible and therefore may be ignored under similar ambient conditions. The total yearly load (cooling plus heating) was found to increase by about 3% for $A_{mj}/A_{tot} = 0.02$ to about 11% for $A_{mj}/A_{tot} = 0.08$, which are the same percentages obtained for the cooling load, as expected. It should also be noted that the percentage increases in loads as a result of thermal bridges obtained from whole building energy analysis are much smaller than the corresponding values obtained from the 2D dynamic study of the transmission load across the wall section, because all other loads are considered in the former analysis, and these loads are almost unaffected by thermal bridges.

The results of this study highlight the importance of the effects of thermal bridges resulting from mortar joints between building blocks. These effects should not be ignored at the design stage, as

they tend to increase design loads and therefore equipment size, and at the operational stage, as they increase the annual energy consumption. Most of the literature on thermal bridges focuses on bridges due to structural elements, while very little attention has been given to mortar joints. It is hoped that this study will fill this gap.

Acknowledgments: This project was funded by the National Plan for Science, Technology and Innovation (MAARIFAH), King Abdulaziz City for Science and Technology, Kingdom of Saudi Arabia, Award Number: 08-ENE376-2.

Author Contributions: The paper is a part of a large research project in the area of energy conservation in buildings. All four authors participated in the planning of this project. The main idea of this particular part of the study was conceived primarily by Sami Al-Sanea through discussions with Mohamed F. Zedan. The paper was written primarily by Mohamed F. Zedan with contributions from Sami Al-Sanea and Abdulaziz Al-Mujahid. Zeyad Al-Suhaibani went through the manuscript and made valuable suggestions, thereby improving the paper. The whole building energy analysis was conducted by Mohamed F. Zedan and verified by Zeyad Al-Suhaibani. The 2D study was conducted mainly by Sami Al-Sanea with some help from Abdulaziz Al-Mujahid and Mohamed F. Zedan.

Conflicts of Interest: The authors declare no conflict of interest. The funding sponsors had no role in the design of the study; in the collection, analyses or interpretation of data; in the writing of the manuscript. However, they encouraged the publication of the results.

Abbreviations

The following abbreviations are used in this manuscript:

2D:	Two-dimensional
3D:	Three-dimensional
ASHRAE:	American Society of Heating, Refrigeration and Air Conditioning Engineers
CDD:	Cooling degree days
HDD:	Heating degree days
HAP:	Hourly Analysis Program
mj:	Mortar joint
MAARIFAH:	Local name in Saudi Arabia for the National Plan for Science, Technology and Innovation
R-value:	Wall thermal resistance
STD:	Standard
TB:	Thermal bridge
TR:	Ton Refrigeration

Appendix A



Figure 1. Picture of an insulated building block.

Appendix B

Table 1. Nomenclature.

Symbol	Meaning
A	heat transfer area (m ²)
c	specific heat (J/kg.K)
H _b	building block height (m)
H _{mj}	mortar joint height (m)
h	heat-transfer coefficient (W/m ² .K)
I _s	solar radiation flux (W/m ²)
k	thermal conductivity (W/m·K)
L	wall thickness (m)
L _{ins}	insulation thickness (m)
N	number of layers in wall
Q	daily or yearly transmission load (kWh/m ² ·day or kWh/m ² ·year)
q	heat flux or instantaneous transmission load (W/m ²)
R _d -value	wall dynamic thermal resistance (m ² ·K/W)
R _n -value	wall nominal (static) thermal resistance (m ² ·K/W)
T	temperature (°C or K)
t	time (s)
x, y	coordinate directions (m)
Greek Letters	
λ	solar absorptivity
ρ	density (kg/m ³)
Subscripts	
c	convection
f	fluid (ambient air)
i	inside
j	layer number in wall
mj	mortar joint
N	inside layer in wall
o	outside
r	radiation
0	initial (t = 0)
1	outside layer in wall

References

1. Al-Sanea, S.; Zedan, M.F. Effect of thermal bridges on transmission loads and thermal resistance of building walls under dynamic conditions. *Appl. Energy* **2012**, *98*, 584–593. [[CrossRef](#)]
2. Hourly Analysis Program (HAP). *Carrier Software Systems*; Hourly Analysis Program: Syracuse, NY, USA, 2011.
3. Sang Soo, A.L. Empirical Validation of Building Energy Simulation Software: DOE2.E, HAP and TRACE. Available online: <http://lib.dr.iastate.edu/rtd/12584> (accessed on 6 January 2016).
4. Al-Tahat, M.; Al-Ali, A. Energy saving opportunities in Jordanian pharmaceutical industries. *Perspect. Innov. Econ. Bus.* **2012**, *10*, 35–50. [[CrossRef](#)]
5. Asdrubali, F.; Baldinelli, G.; Bianchi, F. A quantitative methodology to evaluate thermal bridges in buildings. *Appl. Energy* **2012**, *97*, 365–373. [[CrossRef](#)]
6. Ascione, F.; Bianco, N.; de' Rossi, F.; Turni, G.; Vanoli, G. Different methods for the modelling of thermal bridges into energy simulation programs: Comparisons of accuracy for flat heterogeneous roofs in Italian climates. *Appl. Energy* **2012**, *97*, 405–418. [[CrossRef](#)]
7. Hassid, S. Thermal Bridges across Multilayer Walls: An Integral Approach. *Build. Environ.* **1990**, *25*, 143–150. [[CrossRef](#)]

8. Martin, K.; Erkoreka, A.; Flores, I.; Odriozola, M.; Sala, J.M. Problems in the calculation of thermal bridges in dynamic conditions. *Energy Build.* **2011**, *43*, 529–535. [[CrossRef](#)]
9. Martin, K.; Campos-Celadorb, A.; Escuderoa, C.; Gómezb, I.; Sala, J.M. Analysis of thermal bridge in a guarded hot box testing facility. *Energy Build.* **2012**, *50*, 139–149. [[CrossRef](#)]
10. Evola, G.; Margani, G.; Marletta, L. Energy and cost evaluation of thermal bridge correction in Mediterranean climate. *Energy Build.* **2011**, *43*, 2385–2393. [[CrossRef](#)]
11. Gao, Y.; Roux, J.; Zhao, L.; Jiang, Y. Dynamical building simulation: A low order model for thermal bridges losses. *Energy Build.* **2008**, *40*, 2236–2243. [[CrossRef](#)]
12. Ben-Nakhi, A. Development of an integrated dynamic thermal bridging assessment environment. *Energy Build.* **2003**, *35*, 375–382. [[CrossRef](#)]
13. Bianchi, F.; Pisello, A.; Baldinelli, G.; Asdrubali, F. Infrared Thermography Assessment of Thermal Bridges in Building Envelope: Experimental Validation in a Test Room Setup. *Sustainability* **2014**, *6*, 7107–7120. [[CrossRef](#)]
14. Cuce, E.; Cuce, P. The impact of internal aerogel retrofitting on the thermal bridges of residential buildings: An experimental and statistical research. *Energy Build.* **2016**, *116*, 449–454. [[CrossRef](#)]
15. Lorenzati, A.; Fantucci, S.; Capozzoli, A.; Perino, M. Experimental and numerical investigation of thermal bridging effects of jointed Vacuum Insulation Panels. *Energy Build.* **2016**, *111*, 164–175. [[CrossRef](#)]
16. Quinten, J.; Feldheim, V. Dynamic modelling of multidimensional thermal bridges in building envelopes: Review of existing methods, application and new mixed method. *Energy Build.* **2016**, *110*, 284–293. [[CrossRef](#)]
17. Martins, C.; Santos, P.; da Silva, L. Lightweight steel-framed thermal bridges mitigation strategies: A parametric study. *J. Build. Phys.* **2016**, *39*, 342–372. [[CrossRef](#)]
18. ISO. *Thermal Bridges in Building Construction—Heat Flows and Surface Temperatures—Detailed Calculations*; ISO Standard 10211; ISO: Geneva, Switzerland, 2007.
19. ISO. *Thermal Bridges in Building Construction—Linear Thermal Transmittance—Simplified Methods and Default Values*; ISO Standard 14683; ISO: Geneva, Switzerland, 2007.
20. Owen, M., Ed.; *ASHRAE Handbook of Fundamentals*, American Society of Heating, Refrigerating and Air-Conditioning Engineers, Inc.: Atlanta, GA, USA, 2001.
21. Al-Kasmoul, F.S. Measurements of Thermal Properties of Insulation Materials and Determination of Recommended R-Values for Building Walls. Master’s Thesis, Department of Mechanical Engineering, College of Engineering, King Saud University, Riyadh, Saudi Arabia, 2006.
22. Doggett, S. Climate Data for Building Simulations. Available online: <https://builtenv.wordpress.com/2014/02/27/climate-data-for-building-simulations/> (accessed on 30 May 2016).
23. *American Society of Heating*; ASHRAE Standard 62.1-2007; Refrigerating and Air-Conditioning Engineers, Inc.: Atlanta, GA, USA, 2007.
24. Al-Sanea, S.; Zedan, M.; Al-Mujahid, A.; Al-Suhaibani, Z. *Determination of Optimum R-Values for Building Walls and Roofs under Local Conditions for Use in the Saudi Building Code*; Final Technical Report, Research Project 08-ENE376-2; National Plan for Science and Technology: Riyadh, Saudi Arabia, 2014.
25. The High Commission for the Development of Arriyadh, “About ArRiyadh”. Available online: <http://www.arriyadh.com/ar/AboutArriy/?1=1&menuId=2815> (accessed on 30 May 2016). (In Arabic)
26. Energy Information Administration. *How Much Carbon Dioxide is Produced per Kilowatt-Hour When Generating Electricity with Fossil Fuels?*; Available online: <https://www.eia.gov/tools/faqs/faq.cfm?id=74&t=11> (accessed on 30 May 2016).

